Immunology 1976 **31** 455

Specialized structure and metabolic activities of high endothelial venules in rat lymphatic tissues

N. D. ANDERSON, A. O. ANDERSON* & R. G. WYLLIE *Departments of Pathology, Medicine and Surgery, The Johns Hopkins Medical Institutions, Baltimore, Maryland, U.S.A.*

Received 6 *August* 1975; *accepted for publication* 9 *February* 1976

Summary. Microscopic, histochemical and ultrastructural techniques were used to define characteristics of high endothelial venules (HEV) in rat lymphatic tissues. This endothelium contained acetyl esterase and acid hydrolase activities which were not altered by lymphocyte depletion. No immunoglobulins were detected on luminal surfaces of HEV by fluorescent antibody staining. Only minor structural differences were seen between HEV within lymph nodes and Peyer's patches. At both sites, high endothelial cells were linked together by macular junctional complexes and interlocking basal foot processes. Endothelial cell cytoplasm moulded about surfaces of lymphocytes migrating through the venular wall, and flocculant deposits of basement membrane formed over lymphocytes penetrating the basal lamina. The endothelium was ensheathed by three to five layers of overlapping reticular cell plates and connective tissue. Each plate was linked to the reticular meshwork of the node by collagen bundles and anchoring filaments which inserted into the plate's external limiting membrane. This permitted individual plates to separate or approximate each other as tissue and intravascular pressure varied, and lymphocytes moved across the sheath by insinuating themselves into gaps between overlapping plates. This composite structure of the HEV wall appeared to facilitate lymphocyte entry into the node and minimized vascular leakage.

* Present address: Division of Pathology, U.S. Army Medical Research Institute of Infectious Diseases, Frederick, Maryland 21701, U.S.A.

Correspondence: Dr Norman D. Anderson, Department of Medicine, The Johns Hopkins University, School of Medicine, Baltimore, Maryland 21205, U.S.A.

INTRODUCTION

High endothelial venules (HEV) in lymphatic tissues have been regarded as specialized microvascular structures since their original description by Thomé in 1898. The histological demonstration of numerous lymphocytes in the walls and lumens of these venules lead many investigators (Schumacher, 1899; Schulze, 1925; Hummel, 1935; Dabelow, 1939) to conclude that HEV were important in the exchange of cells between blood and lymphatic tissues. This was substantiated when Gowans (1959) showed that recirculating lymphocytes selectively emigrated from the blood into lymph nodes at this site.

HEV have been reported to possess a characteristic morphology (Clark, 1962; Sugimura, 1964; Claësson, Jorgensen and Röpke, 1971), enzymatic activities (Smith and Henon, 1959; Mikata, Niki and Watanabe, 1968; Röpke, Jorgensen and Claësson, 1972), and surface staining for immunoglobulin G (Sordat, Hess and Cottier, 1971) which were not found in other blood vessels. After Marchesi and Gowans (1964) concluded that lymphocytes passed directly through the cytoplasm of high

endothelial cells to enter the node, other investigators (Goldschneider and McGregor, 1967; Vincent and Gunz, 1970) proposed that the unique structural and metabolic features of this endothelium reflected membrane synthesis and the presence of special transport mechanisms required for intracellular migration. However, this thesis has been challenged by recent ultrastructural studies (Schoefl, 1972; Wenk, Orlic, Reith and Rhodin, 1974) which indicated that lymphocytes migrate intercellularly as they cross this endothelium.

This report describes microscopic, histochemical, immunofluorescence and ultrastructural observations of HEV in normal and lymphocyte-depleted rats. The results indicate that HEV represent specialized venous segments which are constructed to facilitate intercellular lymphocyte migration and minimize vascular leakage.

MATERIALS AND METHODS

Animals

Adult Lewis rats (Microbiological Associates, Walkersville, Maryland) of both sexes weighing between 180 and 250 g were used in these studies.

Anaesthesia

Rats were anaesthetized for all surgical procedures by open-drop ether or intraperitoneal injections with aqueous solutions of chloral hydrate at dosages of 360 mg/kg body weight.

Vascular perfusion techniques

The microvasculature in axillary lymph nodes and Peyer's patches were defined using regional arterial perfusion with alcian blue dye and tissue preparation methods described previously (Anderson and Anderson, 1975).

Thoracic duct cannulation

The thoracic duct was cannulated below the diaphragm using methods described by Gowans (1959). After surgery, the rats were placed in restraining cages, and lymph drainage was maintained for 9–12 days until the daily output of thoracic duct lymphocytes was consistently below 10^8 cells. The general management and fluid replacement of the rats was carried out using techniques outlined by Gowans and Knight (1964).

Preparation of tissue samples

All rats were killed by cervical dislocation. Lymph nodes and Peyer's patches were immediately excised and bissected. One-half of each specimen was snap-frozen in liquid nitrogen and 4 μm cryostat sections were cut for histochemical and fluorescent antibody studies. The remaining halves were prepared for ultrastructural studies. Special fixation methods were utilized to define the ultrastructural changes produced in HEV by increased intravascular or nodal tissue pressure. In some studies, axillary and mesenteric nodes were fixed *in situ* by intra-arterial perfusion with 1·5 per cent glutaraldehyde in 10 per cent dextran–saline solution (adjusted to pH 7·2 with NaOH) after blood had been flushed from the vascular system. In other rats, the lymph nodes were fixed *in situ* by injecting 0·02–0·04 ml of 3 per cent glutaraldehyde directly into the subcapsular sinus to artificially increase intranodal pressure.

Histochemistry

Sections were dried in a vacuum for 10 min before staining. The histochemical methods employed were: lactic and isocitric acid dehydrogenase (Barka and Anderson, 1963), adenosine triphosphatase (Wachstein and Meisel, 1957), acetyl esterase (Davis and Ornstein, 1959), acid phosphatase (Barka, 1960), alkaline phosphatase (Gomori, 1939; Takamatsu, 1939), β-glucuronidase (Hayashi, Nakajima and Fishman, 1964), elastic tissue (Gomori, 1950), and RNA and collagen (Wyllie, personal communication).

Immunofluorescence studies

Two different preparatory methods were used for the immunofluorescence studies. Alternate sections from the same lymph nodes were either air-dried on glass slides and washed three times in cold phosphate-buffered saline (PBS) for 15 min or fixed using techniques described by Sordat *et al.* (1971). These sections were incubated with 1:2–1:8 dilutions of fluorescein-conjugated rabbit anti-rat IgG (Cappel Laboratories, Downingtown, Pennsylvania) for 25 min. Slides were washed three times in fresh PBS and mounted in glycerine for examination with a Zeiss fluorescence microscope using Osram super-pressure mercury lamp HBO 200 W, a u.v. exciter filter, a KG-1 heat-absorbing filter, and a Kodak Wratten 2A gelatin barrier filter.

Electron microscopic techniques

Lymphatic tissues were minced into 1-mm cubes in a drop of cold 3 per cent glutaraldehyde in 0·1 M cacodylate buffer at pH 7·2 and placed in fresh fixative for 2–4 h at 4°. After washing with 3 per cent sucrose in 0·1 M cacodylate, tissues were post-fixed in 1 per cent osmium tetroxide in Millonig's buffer at pH 7·2, dehydrated through graded alcohols to toluene, and embedded in araldite. Sections were cut at 600–900 Å with diamond knives in a Sorval MT-2 ultramicrotome, mounted on uncoated 200-mesh copper grids, stained with aqueous uranyl acetate and/or lead citrate and examined at magnifications ranging from 1600 to 16,000 on an AEI 801 electron microscope.

Cytochemistry

Minced lymph nodes were fixed in 3 per cent glutaraldehyde in 0·1 M cacodylate for 2–4 h at 4° and washed overnight in 3 per cent sucrose in 0·1 M cacodylate (pH 7·3). Smith–Farquhar chopper sections were cut at 50 μm and washed in 7·5 per cent sucrose for 30 min. Sections were incubated in Gomori's lead salt mixture for acid phosphatase, osmicated, and embedded as described by Anton, Brandes and Barnard (1969). The distribution of acid phosphatase reaction product was determined in unstained 1 μm sections examined at 80 kV with an AEI 801 electron microscope. Adenosine triphosphatase (ATPase) activity was identified on sections prepared in the same manner using Wachstein–Meisel lead medium, the disodium salt of ATP as the substrate and magnesium as the activating ion (Novikoff, Essner, Goldfischer and Heus, 1962).

RESULTS

Macrostructure of high endothelial venules

Cleared slices were examined from more than fifty lymph nodes and Peyer's patches stained *in vivo* by regional infusions with alcian blue dye. HEV were readily identified by their characteristic 'double outline' staining pattern produced by deposition of alcian blue on endothelial surfaces and the underlying basement membrane (Fig. 1). When the luminal surfaces of the venules were viewed *en face*, small indentations or apical gaps were frequently seen between margins of adjacent endothelial cells (Fig. 2). In lymph nodes, HEV appeared to be randomly distributed in cortical lobules. The main trunk of each venule received three to five smaller side branches as it coursed from beneath the marginal sinus through the cortex. The main segments of these HEV were located within the diffuse cortex between secondary follicles, but their smaller side branches occasionally appeared juxtaposed to, or displaced by, the outer margins of expanding follicles. Short segments of small venules lined by flat endothelium were interposed between capillary beds and HEV (Figs 3–5). Capillaries were never seen emptying directly into HEV, but these venules were directly linked to the arterial circulation by three to eight arteriovenous communications which looped through the outer cortical capillary arcade. In the medulla, the venules merged into larger, segmental veins (Figs 4 and 5). Focal, circumferential constrictions of the venular wall were seen in segmental veins where they joined larger efferent vessels near the hilus.

The small intestinal wall contained small vessel plexuses situated in the serosa, submucosa, and lamina propria at the base of the villi. This venous pattern was modified near Peyer's patches where HEV formed a freely anastomosing network in the interfollicular (T-cell) regions (Fig. 6). These HEV located above the muscularis mucosa received small venules from the adjacent lymphatic parenchyma and overlying muscles. Short, vertical trunks lined by high endothelium linked the venules to other HEV located just beneath the muscularis mucosae. This plexus drained into large veins lined by flat endothelium. At the margins of Peyer's patches, the veins passed through the muscularis propria to join with larger efferent vessels of the mesenteric system. Venules in the lamina propria were lined by flat endothelium, but some HEV extended through the muscularis mucosae to merge with capillary beds at the base of intestinal crypts. Long segments of the anastomosing HEV within Peyer's patches had luminal diameters which were 2–3 times wider than those seen in HEV of axillary lymph nodes. The outer plexus of HEV was directly linked to the arterial circulation by several arteriovenous communications.

Microstructure of high endothelial venules

In toluidine blue-stained thick sections of lymph nodes, HEV were easily identified by their cuboidal endothelial cell lining, the presence of infiltrating

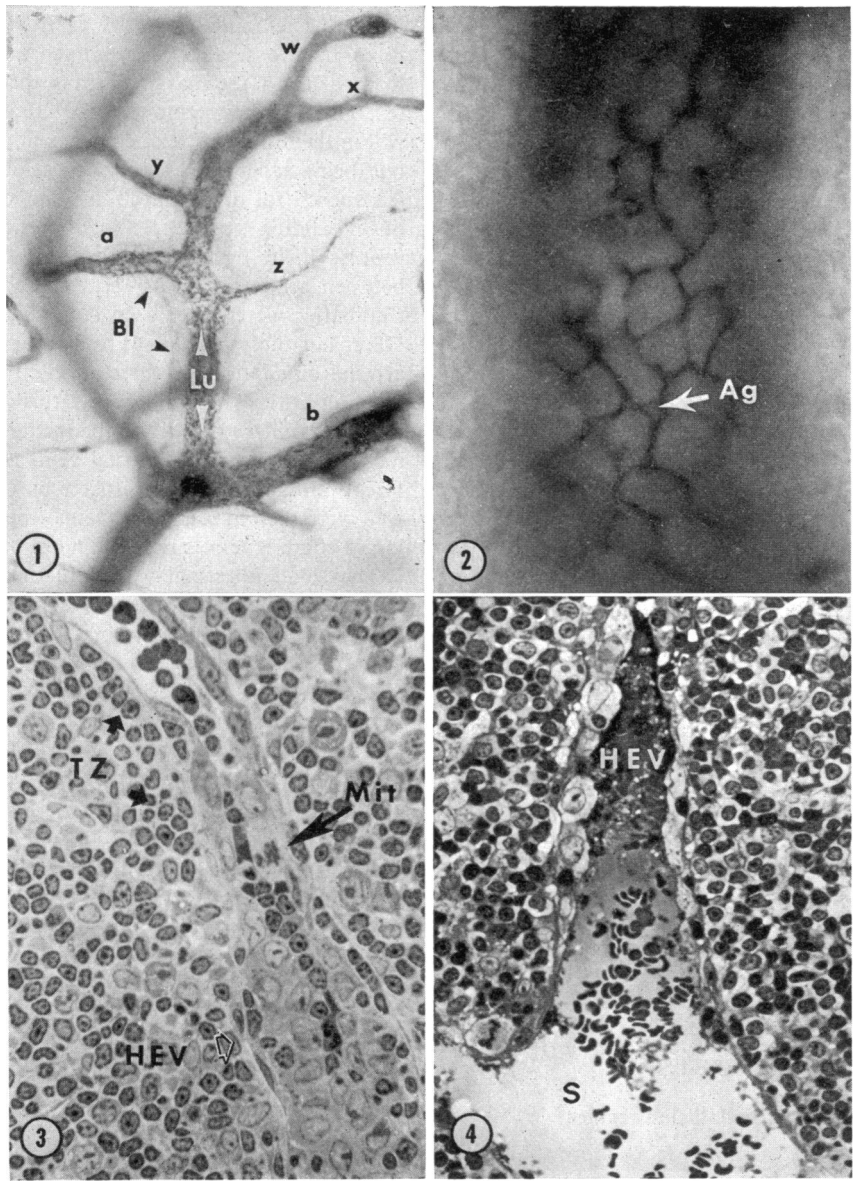

Figure 1. Distinctive appearance of high endothelial venules (HEV) in cleared lymph node sections where the vasculature was stained *in vivo* by regional perfusion with Alcian blue. This dye stains luminal (Lu) and basal (Bl) surfaces of endothelial cells lining these venules and the double outline facilitates identification of HEV. Two high endothelial side branches (a and b) and four low endothelial venules (w, x, y, z) join with the main trunk. (Magnification × 184.)

Figure 2. Viewed *en face*, HEV display a characteristic 'cobblestone' staining pattern in this cleared section. Apical gaps (Ag) are seen between margins of adjacent endothelial cells. (Magnification × 792.)

Figure 3. Proximal transition zone (TZ) at the junction between a venule lined by low endothelium and a HEV. A mitotic figure (Mit) is seen within a high endothelial cell at this site. (Toluidine blue; magnification × 560.)

Figure 4. Gradual transition from high to low endothelium at the corticomedullary junction where this HEV merges into a lobular vein (S). (Toluidine blue; magnification × 560.)

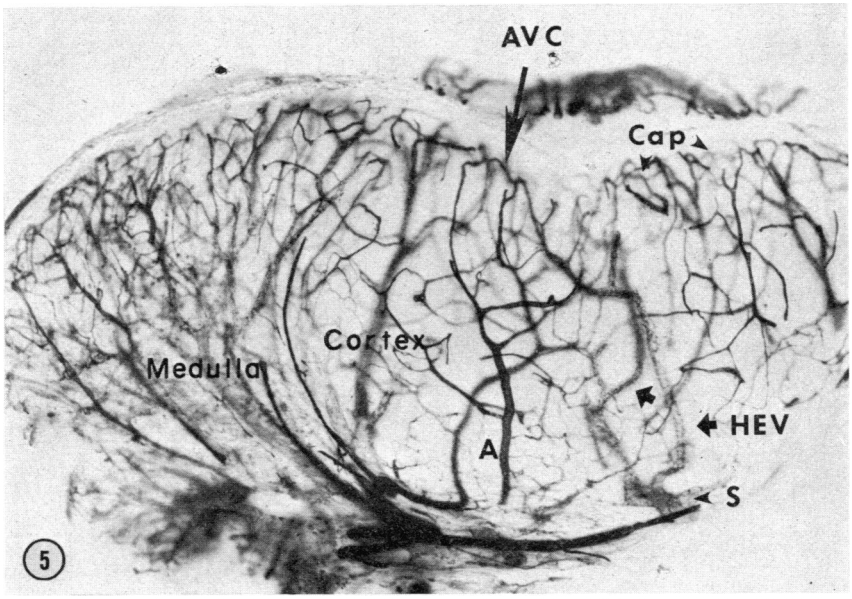

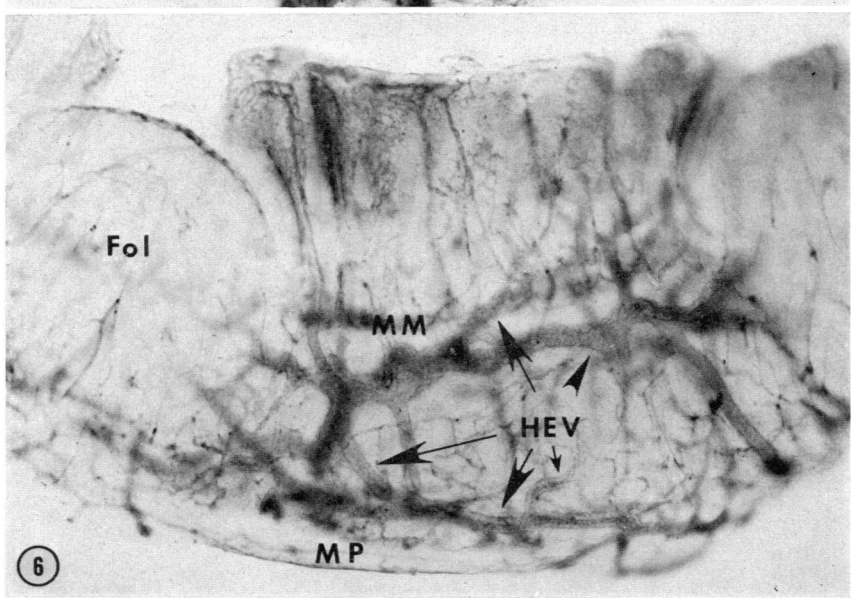

Figure 5. In this 150-μm section of cleared lymph node, arteries (A) show increased staining density due to post-excisional contraction. Arteries enter at the hilus and continue to arborize as they pass into the cortex where they terminate in capillary beds (Cap). Arteriovenous communications (AVC) form loops beneath the marginal sinus and join directly with HEV which drain into segmental veins (S) in the medulla. Rich capillary arcades are seen about medullary cords. (Magnification × 42.)

Figure 6. In Peyer's patches, HEV form a freely anastomosing network in the interfollicular regions. Venous plexuses situated near the muscularis propria (MP) and muscularis mucosa (MM) are joined by short, perpendicular venous segments. Some HEV pass through the muscularis mucosa and merge with capillary beds at the base of intestinal crypts. Relatively few blood vessels are seen in the adjacent follicle (Fol). (Magnification × 57.)

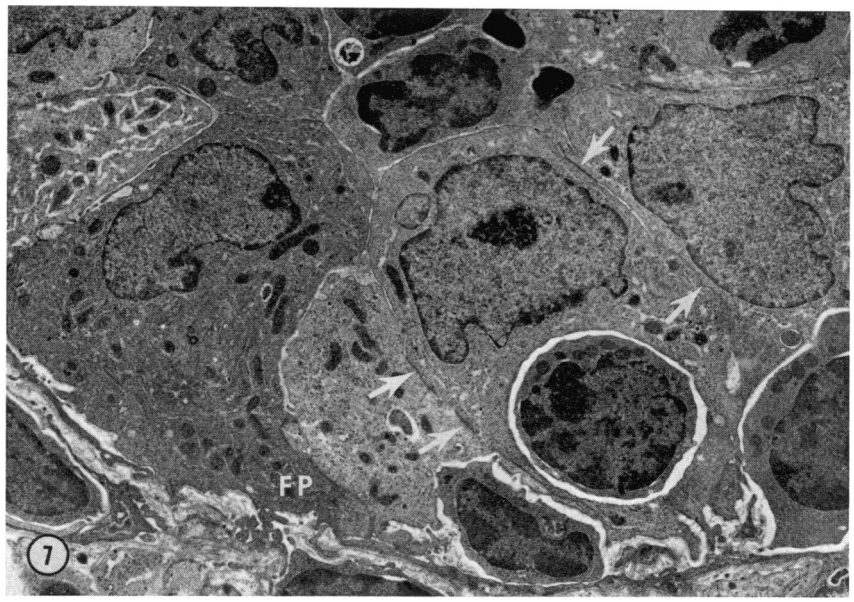

Figure 7. In normal lymph nodes HEV are lined with columnar endothelial cells of two morphological types. In most cells the abundant cytoplasm exhibits faint electron density, but occasional cells contain dense cytoplasm. The high endothelial cells are linked together by apical and basilar junctional complexes (arrows). Foot processes (FP) extend beneath adjacent endothelial cells. (Lead citrate; magnification × 4000.)

Figure 8. In Peyer's patches, HEV are lined by cuboidal endothelial cells which possess cytoplasmic characteristics similar to those seen in lymph nodes. Apical junctional complexes are absent in this endothelium and the basal foot processes (FP) are shorter than those seen in Fig. 7. The perivenular sheath (RCS) is composed of three to five layers of reticular cell plates separated by thick bundles of collagen and amorphous ground substance. (Lead citrate; magnification × 4000.)

lymphocytes, and the surrounding reticular sheath (Fig. 3). Longitudinal sections through HEV showed that these vessels progressively increased in size as they passed through the cortex. Their luminal diameter varied from 6 to 8 μm near their origin to greater than 30 μm at the corticomedullary junctions (Fig. 4). There was an abrupt transition from flat to cuboidal endothelium where small venules joined HEV in the cortex which contrasted with the irregular conversion from polygonal to flat endothelium seen as HEV merged with lobular veins near the medulla.

In electron micrographs, these endothelial cells could be separated into two morphological types by variations in cytoplasmic density and functional differentiation of organelles (Fig. 7). Most of the endothelial lining was composed of large cells with faintly electron-dense cytoplasm containing a prominent Golgi apparatus, six to eight elongated mitochondria, numerous free and clustered ribosomes, and sparse endoplasmic reticulum. Their luminal surfaces were usually smooth; occasional pinocytotic vesicles were seen invaginating from lateral borders of the cell membrane. One or two multivesicular bodies were found in the cytoplasm, but typical Wiebel-Palade bodies were not seen. These endothelial cells contained two or three residual bodies with characteristic crystalline and globular osmiophilic inclusions. Their large, lobular nuclei displayed loose chromatin which condensed at the periphery, ten to twelve nuclear pores and one or two prominent nucleoli. Interspersed in the population were other endothelial cells with increased cytoplasmic density caused by an abundance of polyribosomes and rough endoplasmic reticulum

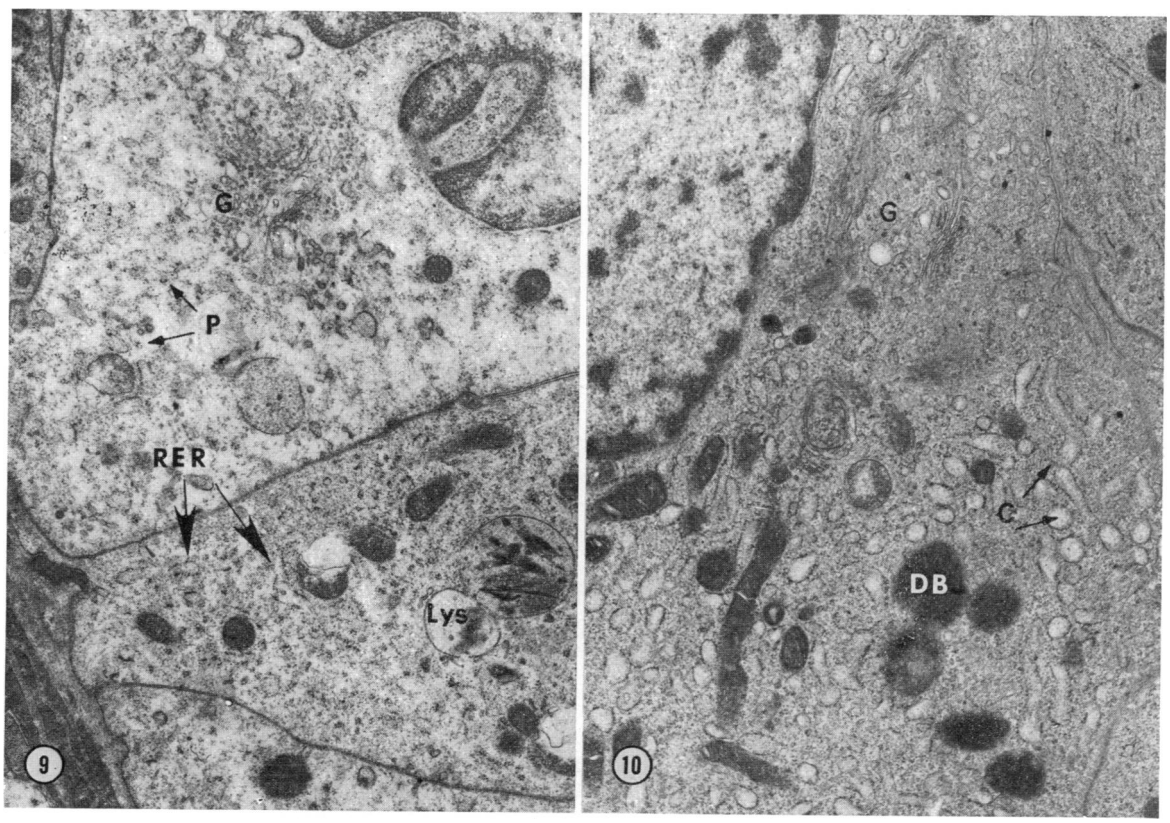

Figure 9. The typical morphology of 'light' endothelial cells in HEV. The cytoplasm contains: a prominent golgi (G), dispersed polyribosomes (P), sparse rough endoplasmic reticulum (RER), and residual lysosomes (Lys) containing crystalline and amorphous inclusions. (Lead citrate; magnification × 14,000.)

Figure 10. The cytoplasm of this 'dark' endothelial cell contains numerous polyribosomes, RER cysternae (C) and dense bodies (DB). (Lead citrate; magnification × 14,000.)

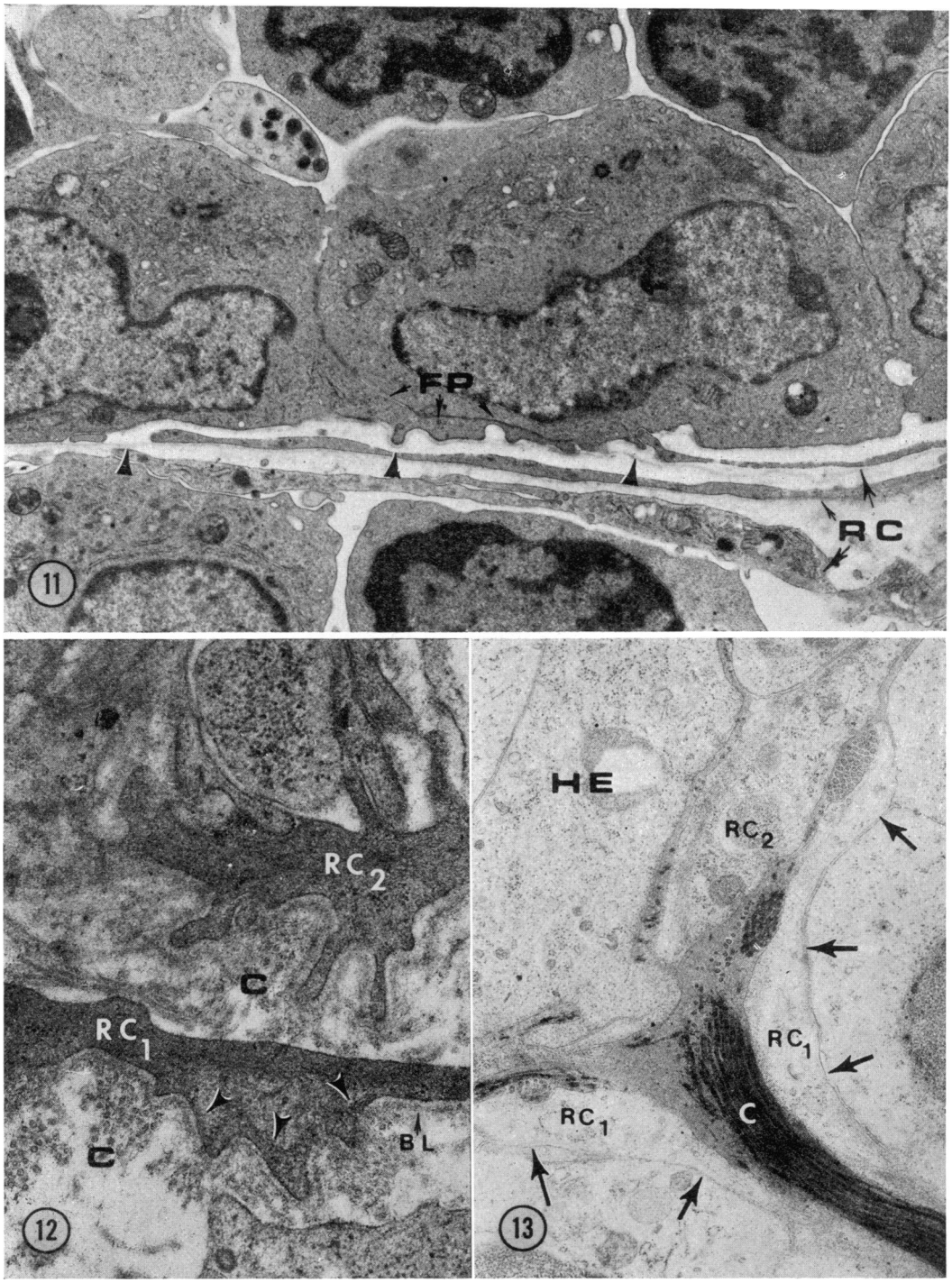

Figure 11. The structure of the HEV wall. A thin basal lamina (arrows) follows abluminal contours of endothelial cells and divides to cover the outer surfaces of reticular cell plates (RC) in the perivenular sheath. A basal foot process (FP) extends beneath an adjacent endothelial cell. (Lead citrate; magnification × 9000.)

Figure 12. Collagen bundles (C) are seen inserting into the basement membrane (BL) covering outer surfaces of reticular cell plates (RC). Cytoplasmic microfibrils (arrows) abut the reticular cell plasmalemma at these sites. (Lead citrate; magnification × 25,000.)

Figure 13. The collagen (C) and ground substance of a reticular fibre is seen inserting in the perimeter of the reticular cell sheath (RC 1 and 2) of the HEV. The abluminal portion of a high endothelial cell (HE) is shown. The covering of the reticular fibre also spreads out over the RC to form its cytoplasmic plates (arrows). (Uranyl acetate and lead citrate; magnification × 14,000.)

Figure 14. Intra-arterial perfusion fixation causes HEV endothelial cells to flatten and obliterate intercellular spaces. The layers of reticular cell plates (RC) in the laminated sheath approximate each other and seal gaps between their overlapping margins. (Lead citrate; magnification × 7600.)

Figure 15. Intralymphatic injections of fixative results in apparent flow (solid arrows) from the node interstitium across the walls of HEVs. This separates reticular cell plates (RC) and widens spaces (asterisks) between endothelial cells and migrating lymphocytes. (Lead citrate; magnification × 6040.)

(Fig. 10). Numerous folds projected from luminal surfaces of these cells. Their cytoplasm contained dense bodies, mitochondria with dense matrices and dilated Golgi saccules while their nuclei showed irregular borders, eccentric nucleoli and numerous nuclear pores.

These polygonal cells formed a continuous endothelial lining where individual cells were separated by oblique intercellular gaps measuring 200–400 Å. Adjacent cells were joined together by macular tight junctions located near their luminal and basal surfaces (Figs 7–11). Occasionally, mid-portions of these cells were linked by interlocking cell processes. The apical junctional complexes were usually absent in distal HEV segments near transition zones and this resulted in wider and deeper (1000–10,000 Å) clefts between endothelial cells at these sites. Foot processes extended from basilar portions of endothelial cells and entered the perivascular sheath where they formed junctions with reticular cell processes. A thin basal lamina followed abluminal contours of the endothelium, and divided to cover external surfaces of these reticular cell processes. Collagen fibres were closely applied along the outer surface of the basal lamina near junctions between endothelial cells.

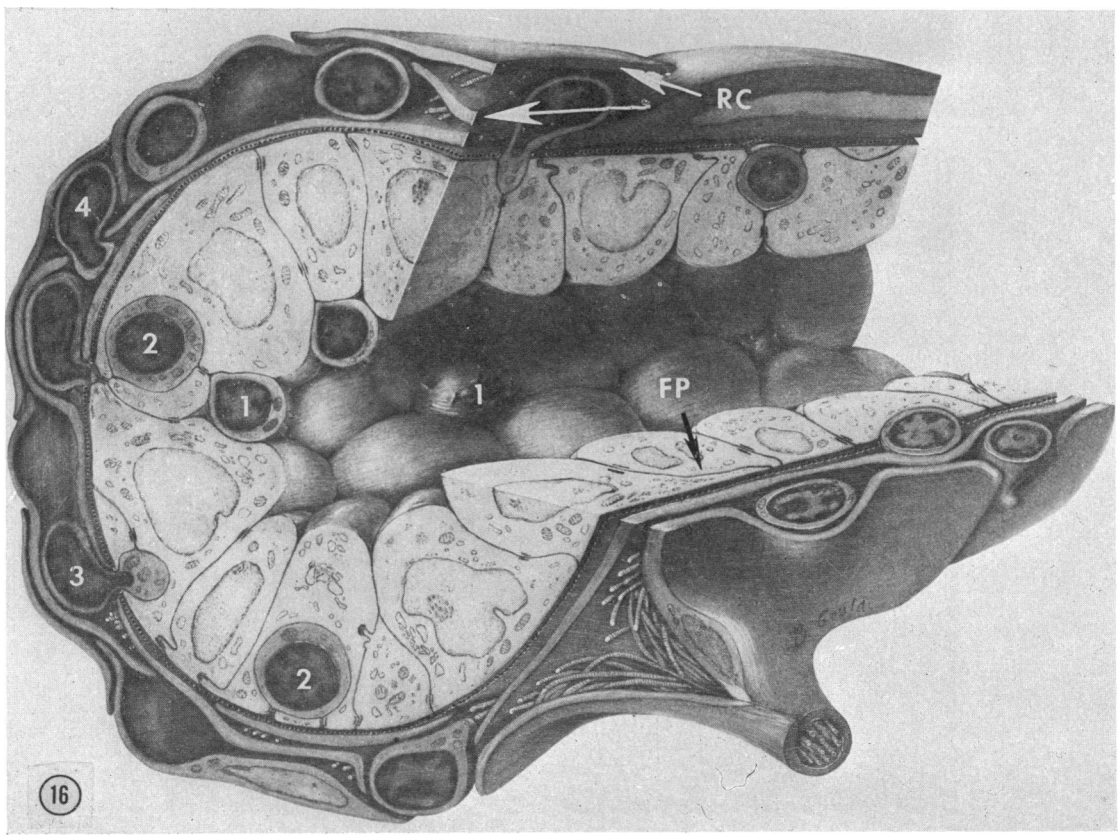

Figure 16. Composite view of the structure of HEV in rat lymph nodes. HEV are lined by polygonal endothelial cells which are joined to each other by apical and basilar junctional complexes. Basal foot processes (FP) extend for varying distances beneath adjacent endothelial cells. This endothelium rests upon a delicate basement membrane (dotted line) which also invests the outer surfaces of reticular cell plates in the surrounding sheath. The perivenular sheath is composed of three layers of overlapping reticular cell plates (RC). Each plate is individually 'guy-wired' by collagen bundles to the reticular framework of the node. The sequence of lymphocyte migration across this venular wall is illustrated. Lymphocytes are shown: adhering to luminal surfaces of the endothelium (1); moving through intercellular spaces between endothelial cells (2); crossing the basement membrane (3) and traversing successive laminations of the reticular cell sheath (4). (Magnification × 3200.)

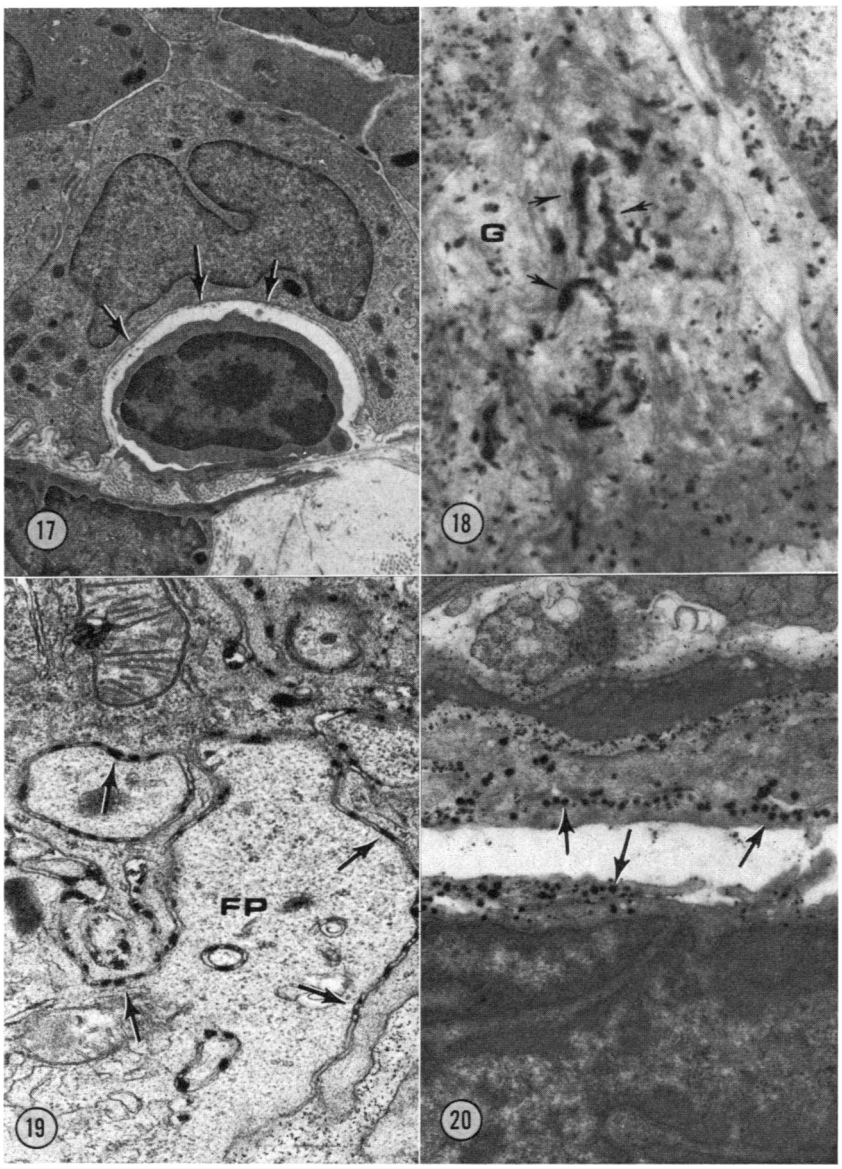

Figure 17. Flocculent deposits of basement membrane material (arrows) are found along the endothelial cell membrane surrounding this migrating lymphocyte which lies between the endothelial cell and the reticular cell sheath. (Lead citrate; magnification × 6560.)

Figure 18. Acid phosphatase activity (arrows) is seen localized within Golgi saccules (G) of high endothelial cells. Unstained 0·5 μm section incubated in Gomori's lead salt mixture. (Magnification × 32,000.)

Figure 19. Adenosine triphosphatase activity (arrows) in high endothelial cells is concentrated along outer surfaces of abutting foot processes (FP), and within cytoplasmic vesicles. (Wachstein–Meisel lead–salt medium for ATPase counterstained *en bloc* with uranyl acetate; Magnification × 25,000.)

Figure 20. Adenosine triphosphatase activity is seen within pinocytotic vesicles (arrows) along luminal surfaces of flat endothelial cells lining terminal arterioles. (Wachstein-Meisel lead–salt medium for ATPase without counterstaining; magnification × 13,600.)

HEV were surrounded by complex, connective tissue sheaths (Figs 11–15) which spiralled about the entire length of these venules and ended abruptly at transitions from high to low endothelium. Serial thin sections demonstrated that the sheath was formed by two or three layers of overlapping, cytoplasmic plates derived from reticular cells. The dense cytoplasm forming these plates contained numerous ribosomes, mitochondria and peripherally-situated parallel bundles of microfibrils. Collagen bundles inserted into the basement membrane covering outer surfaces of these plates at sites where adjacent microfibrils abutted the plasmalemma (Fig. 12). These collagen bundles individually linked each layer of reticular plates to the supporting stroma of the node (Fig. 13). This anchoring mechanism permitted reticular plates to separate or approximate in response to local pressure changes. When intravascular pressure was increased by perfusion-fixation with glutaraldehyde, HEV were moderately distended. This caused adjacent endothelial cells to flatten over each other, and overlapping margins of the surrounding reticular plates were tightly opposed (Fig. 14). This effectively sealed potential gaps in the endothelium and the laminated sheath. Direct injection of fixatives into the node produced enlarged extracellular spaces between endothelial cells and wide separation of reticular cell plates in the sheath (Fig. 15).

In normal lymph nodes, lymphocytes were seen at all levels within HEV walls (Fig. 16). Endothelial cell cytoplasm appeared to mould closely about lymphocytes moving through intercellular spaces excluding other blood elements from these channels. Flocculent deposits of basement membrane material covered surfaces of lymphocytes crossing the basal lamina (Fig. 17). Lymphocytes infiltrated potential spaces between layers of the reticular sheath, and appeared to migrate radially across successive laminations by insinuating themselves through gaps between overlapping reticular plates (Fig. 16). Occasional lymphocytes were seen entering the nodal interstitium at sites where the reticular sheaths terminated in the outer cortex.

HEV within Peyer's patches exhibited only minor structural differences from those seen in lymph nodes. These venules frequently had luminal diameters measuring from 40 to 80 μm, but progressive luminal narrowing and abrupt transition from polygonal to flat endothelium were observed in side branches. The high endothelial cells exhibited a relatively uniform appearance by light microscopy, but could be classified into two types by ultrastructural variations in their nuclear morphology and content of cytoplasmic organelles. These cells lacked apical junctional complexes and were separated by deep clefts of irregular width in which lymphocytes were frequently seen emigrating in clusters. The surrounding perivascular sheaths were composed of three to five concentric layers of reticular cell plates which were separated by amorphous ground substance containing thick bundles of collagen. Numerous lymphocytes were present in the laminated sheath and processes from tissue macrophages frequently extended into gaps between the outer layers of reticular plates.

Table 1. Comparative enzymatic activities of the endothelium in lymph node blood vessels

Enzymes	Intensity of reaction*			
	High endothelial venule	Medullary veins	Capillaries	Arterioles
Lactic dehydrogenase	++	++	++	++
Isocitric dehydrogenase	++	++	++	++
Adenosine triphosphatase	+	++	++	++
Alkaline phosphatase	0	0	++	+++
Acetyl esterase	+++	0	0	0
Acid phosphatase	+	0	0	0
β-Glucuronidase	+	0	0	0
Cytoplasmic RNA	++	0	0	0

* Recorded as ++++ = intense activity, +++ = strong activity, ++ = moderate activity, + = weak activity, and 0 = no activity.

Histochemical and cytochemical staining of high endothelial cells

Histochemistry was used to compare metabolic activities in high endothelial cells with staining reactions seen in other blood vessels (Table 1). All types of endothelium showed moderate to intense staining for lactic dehydrogenase, isocitric dehydrogenase and ATPase activity. When cytochemical techniques were employed to localize ATPase activity, reaction product was distributed between outer surfaces of cell membranes of adjacent basal foot processes and within coated vesicles scattered throughout high endothelial cell cytoplasm (Fig. 19). In arteriolar endothelial cells, ATPase reaction product localized within pinocytotic vesicles located near the luminal surface (Fig. 20). The endothelium in arterioles and capillaries displayed alkaline phosphatase activity which was not present in venules lines by either flat or polygonal cells. HEV showed variable cytoplasmic staining with methyl green–pyronin, but similar pyroninophilia was not seen in flat endothelial cells. All high endothelial cells exhibited diffuse cytoplasmic staining for acetyl esterase activity. Examination of ninety-two and sixty-four sequential serial sections through two different axillary nodes demonstrated considerable variation in staining intensity between different cells in the same venule, but all HEV segments stained for acetyl esterase activity and this abruptly terminated at transition sites from high to low endothelium. In addition, high endothelial cells showed light to intense staining for acid phosphatase and β-glucuronidase activity. Cytochemical techniques localized this acid phosphatase activity within prominent Golgi saccules, Golgi-associated vesicles and in RER segments adjacent to the convex face of the Golgi (Fig. 18). There was no indication that acid phosphatase surrounded lymphocytes which appeared incarcerated within endothelial cell cytoplasm, or that acid phosphatase-containing vesicles emptied into extracellular spaces where lymphocytes were migrating between cells. Aldehyde fuchsin stains demonstrated that numerous strands of elastic fibres surrounded the large segmental veins and extended for short distances into the connective tissue adjacent to terminal HEV segments. The perivascular sheath surrounding other HEV segments was devoid of elastic tissue but did contain a thin (1 μm), irregular meshwork of collagen bundles demonstrable by fast green–safranin stains.

HEV within Peyer's patches showed similar metabolic characteristics. The only consistent differences noted were that many of these high endothelial cells displayed β-glucuronidase staining of greater intensity than that seen in normal axillary nodes, and the thick perivascular sheath contained numerous elastic fibres in addition to dense collagen bundles.

Localization of IgG in high endothelial venules

Immunofluorescence studies were made on twelve normal axillary nodes and eight regional nodes excised 7 days after stimulation by local injections of 0·1 ml of alum-precipitated tetanus toxoid or by skin allografting. When unwashed, fixed cryostat sections from these nodes were incubated with fluorescein-conjugated rabbit anti-rat IgG, specific staining of variable intensity was seen along apical and lateral borders of high endothelial cells and within granular

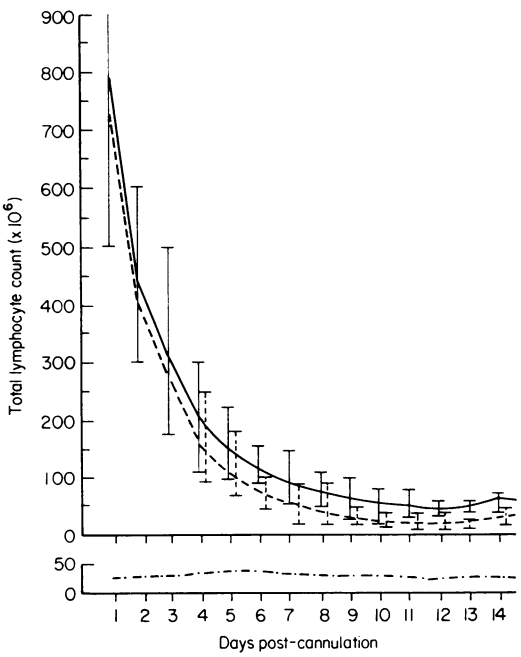

Figure 21. Daily loss of lymphocytes from chronic thoracic duct fistulae in adult rats. Brackets define the range of lymphocyte output observed in individual animals at each day of lymph drainage. The daily output of small lymphocytes (smaller than 8 μm) (– – –) rapidly declined during the initial drainage period and continued at reduced, but relatively constant levels after 6 days. The daily output of large lymphocytes (greater than 8 μm) (– · – ·) was maintained at a constant low level throughout the 14-day study period. Total number of cells (———).

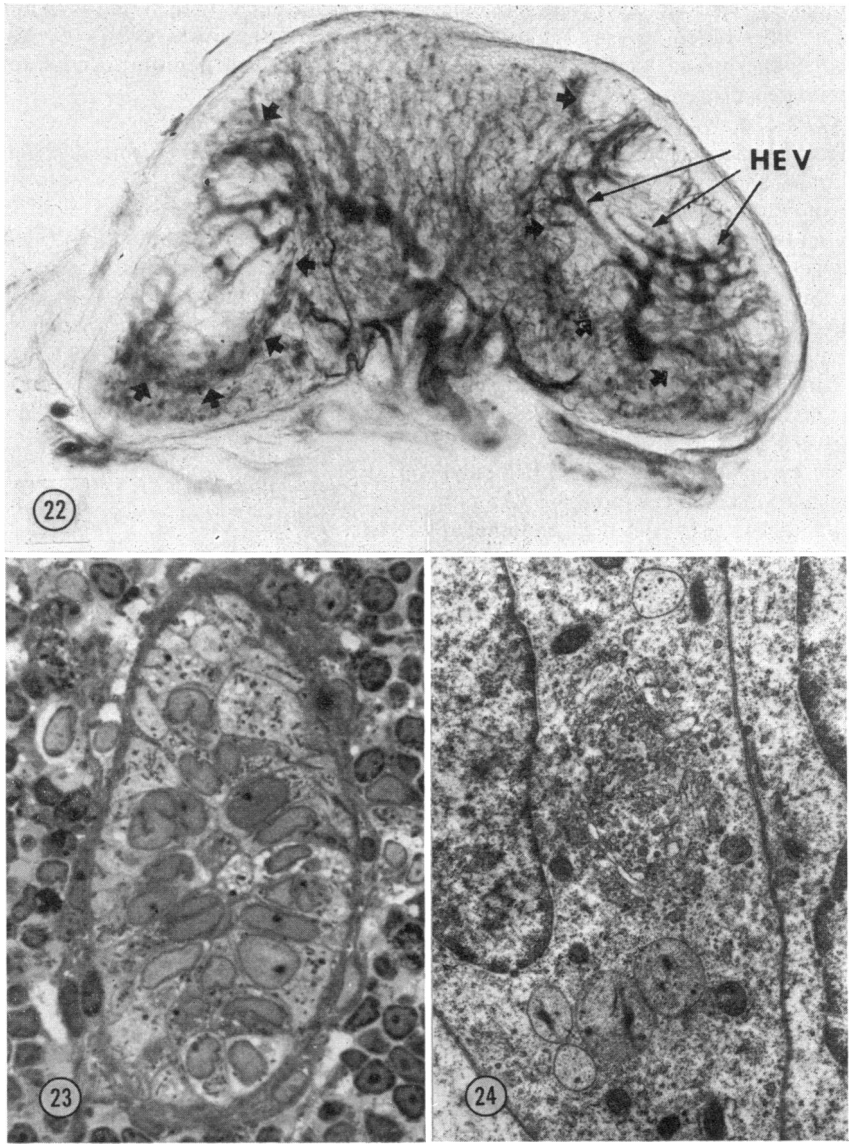

Figure 22. This cleared section of an axillary lymph node excised after 12 days of lymph drainage shows reduced cortical mass (arrows). This is accompanied by compression and increased tortuosity of the cortical vasculature. Typical HEV are seen in the condensed cortex. (Magnification × 53.)

Figure 23. High endothelial cells retain their characteristic polygonal shape in this node removed from a rat subjected to 8 days of thoracic duct drainage. Note the absence of migrating lymphocytes. (Toluidine blue; magnification × 720.)

Figure 24. High endothelial cells maintain abundant cytoplasm and their usual complement of organelles after lymphocyte depletion was produced by 12 days of lymph drainage. (Lead citrate; magnification × 14,400.)

precipitates in the lumens of HEV, arterioles and veins. Fluorescence on the HEV wall was decreased markedly or absent in alternate sections which had been washed for 30 s in PBS prior to fixation. Similar studies using unfixed sections washed for 15 min before staining failed to demonstrate immunoglobulin within the lumen or on the surface of HEV. The only vessels showing positive reactions for surface IgG in such preparations were small venules which measured 10–15 μm in diameter and were lined by four or five endothelial cells in cross sections. No migrating lymphocytes were seen in the walls of these vessels.

Microvascular changes in nodes of lymphocyte-depleted rats

Continuous thoracic duct drainage was maintained through Bollman-type fistulas for 8–12 days. Rats were killed for morphologic studies when their daily output of thoracic duct lymphocytes had fallen below 10^8 cells for 2–4 consecutive days (Fig. 21). This produced profound lymphocyte depletion manifested by more than 50 per cent reduction in axillary node weight and histologic evidence of striking cellular depletion in the deep cortex of these nodes. Regional perfusions with alcian blue dye demonstrated distorted angioarchitecture in each node (Fig. 22). Despite changes in nodal volume, arteries and veins in the hilus and medulla maintained their typical morphology and lobular distribution. This appeared consistent with histological findings indicating that cellular populations in the medulla were unaltered by protracted thoracic duct drainage. However, marked cellular depletion in the cortex was accompanied by increased tortuosity and dilatation of small arteries and veins beneath the subcapsular sinus. Terminal loops within the vascular arcades formed glomerulus-like structures around residual follicles in the cortex. Typical HEV were seen extending from the outer cortex to the corticomedullary junction in all nodes. These vessels showed some increased tortuosity and were grouped more closely within the condensed cortex.

Light microscopy revealed a characteristic pattern of lymphocyte depletion in these nodes. The subcapsular sinus was virtually devoid of lymphocytes, and the remaining cortex was reduced to a rim of compact reticular cells and scattered lymphocytes. A few small follicles were found in the outer cortex and were surrounded by condensed networks of capillaries, small venules and arterioles. The paracortex was markedly depleted of lymphocytes leaving the bulk of the node composed of medullary cords crowded with plasma cells. HEV were present in increased numbers within each high power field of cortical tissue examined, but few lymphocytes remained within their lumens, walls or perivascular sheaths (Fig. 23). Electron microscopy showed that high endothelial cells retained their abundant cytoplasm and characteristic organelles despite the paucity of migrating lymphocytes (Fig. 24). The few lymphocytes seen migrating from HEV tended to have more cytoplasm and well developed Golgi apparatus. The perivascular sheaths contained small numbers of lymphocytes and a relative increase in monocytes.

Histochemistry showed that high endothelial cells within depleted nodes retained the characteristic cytoplasmic basophilia, nonspecific esterase and acid hydrolase activities seen in normal rats. Occasional HEV showed increased staining for acid phosphatase and ATPase activities. Aldehyde fuchsin stains demonstrated irregular condensation and increased tortuosity of elastic fibres within the collapsed cortical stroma.

DISCUSSION

Several investigators have proposed that HEV represent specialized vascular units which regulate fluid and cellular exchange between lymphatic tissues and blood. Schulze (1925) first described HEV as leaky vessels lined by loose-fitting endothelial cells which formed patent stomata for the passage of lymphocytes. After demonstrating that HEV were not highly permeable to particulate dyes, Dabelow (1939) suggested that the increased height of these endothelial cells might permit them to close about lymphocytes migrating through intercellular spaces and this would allow lymphocytes to cross the endothelium like 'ships in canal locks' with minimal vascular leakage. This hypothesis was supported by ultrastructural studies indicating that the plastic cytoplasm of high endothelial cells moulded about the surfaces of lymphocytes migrating intercellularly (Schoefl, 1972; Wenk *et al.*, 1974).

The present study suggests that the entire wall of HEV and their surrounding reticular sheaths can be regarded as structural adaptations for regulating fluid and cellular transport in the node. HEV were lined by polygonal endothelial cells linked together

by discontinuous junctional complexes. Lymphocytes migrated through potential spaces between adjacent endothelial cells without separating these junctions by displacing endothelial cell cytoplasm. As lymphocytes moved toward the basilar portion of HEV, the luminal surfaces of endothelial cells reverted to their original shape, preventing other blood elements from entering the intercellular clefts. Basement membrane appeared to reform over lymphocyte surfaces to seal gaps made by these migrating cells as they penetrated the basal lamina. HEV were surrounded by a laminated sheath composed of layers of overlapping reticular cell plates. This provided support of the venular wall and permitted lymphocytes to move longitudinally between layers or migrate radially across the sheath through gaps between reticular plates. Since the sheath extended from the outer cortex to the corticomedullary junction, potential channels in this laminated structure could serve as conduits for directing migrating lymphocytes to T and B cell zones of the node as suggested by Söderström (1967). In addition, each layer of the sheath was individually linked to structural members of the lymph node reticulum through anchoring filaments which inserted in the sheath cell plasmalemma. This pattern of construction was analogous to that described in lymphatic capillaries (Leak and Burke, 1968), and permitted overlapping reticular plates to separate or approximate each other with changes in interstitial and intravascular pressure. This could provide valve-like functions regulating movement of fluid and cells. In nodes subjected to inflammatory stimuli, increased interstitial fluid pressure might cause these plates to separate enhancing radial migration of motile lymphocytes across the sheath and facilitating movement of fluid and macromolecules from the node towards the venular lumen. Similar movement of fluid, macromolecules and cells could be impaired when intravascular pressures exceeded tissue pressure and closed gaps between the overlapping plates. Since HEV are subject to regional haemodynamic controls which cause wide variations in intravascular pressure (Anderson and Anderson, 1975), this unique structure of the venular wall and its surrounding sheath provides an anatomical basis for functional lymph node-venous communications proposed by other investigators (Pressman *et al.*, 1962; Fukuda, 1968).

Other reports (Schulze, 1925; Hummel, 1935; Marchesi and Gowans, 1964) concluded that HEV were lined by specialized endothelial cells which were qualitatively different from other types of endothelium. This study confirmed previous ultrastructural descriptions (Clark, 1962; Sugimura, 1964) indicating that most high endothelial cells exhibited abundant cytoplasm containing a prominent Golgi, coated and uncoated vesicles, numerous free and clustered ribosomes, variable RER, several mitochondria and a few residual lysosomes. Occasional cells showed nuclear and cytoplasmic organelle changes consistent with increased RNA and protein synthesis. Jorgensen and Claësson (1972) described similar ultrastructural variations in HEV of neonatally thymectomized mice and proposed that this represented an early stage of cellular degeneration associated with wasting disease. However, the demonstration of comparable cells in normal and stimulated nodes (Anderson, Anderson and Wyllie, 1975) suggests that these morphological differences reflect physiological variations in endothelial cell function.

Several investigators (Smith and Henon, 1959; Röpke *et al.*, 1972) have found metabolic activities in HEV which were scanty or absent in other blood vessels. Suggestions that high endothelial cells might possess distinctive capabilities for shifting from aerobic to anaerobic metabolism (Röpke *et al.*, 1972) have never been substantiated. The present study demonstrated lactic and isocitric dehydrogenase activities, required for transfer processes in the Embden-Meyerhoff and Krebs cycle pathways, in the endothelium of all lymph node blood vessels. ATPase activity was found in arteriolar smooth muscle and all types of endothelial cells. The significance of the cytochemical localization of this enzyme within pinocytotic vesicles and spaces between HEV basal foot processes is uncertain, but there was no evidence that reaction product deposited about contractile proteins in endothelial cells as postulated by Becker and Nachman (1973). The endothelium of arterioles and capillaries in lymph nodes exhibited positive reactions for alkaline phosphatase; this enzymatic activity was not found in venules. Since similar staining patterns have been observed in other vascular beds (Romanul and Bannister, 1962), this difference could not be attributed to unique functions of HEV. Nonspecific esterase activity appeared to be a characteristic metabolic marker for high endothelial cells (Smith and Henon, 1959; Röpke *et al.*, 1972) since it was found in every HEV and could not be detected in other blood vessels. The

differences in staining intensity between individual cells in the same venule supported ultrastructural findings suggesting that high endothelial cells were in different functional states. However, the significance of these observations remains uncertain as non-specific esterases are poorly characterized enzymes which degrade a variety of different substrates. Although acetyl esterase activity has been identified within lysosomes (Davis and Ornstein, 1959), it seemed unlikely that the diffuse cytoplasmic staining could be attributed to the small number of residual lysosomes seen in high endothelial cells.

There has been considerable debate over the presence of acid hydrolase activity in high endothelial cells. Smith and Henon (1959) were unable to demonstrate lysosomal enzymes in HEV of normal mice. Röpke *et al.* (1972) described diffuse cytoplasmic staining for acid phosphatase in HEV within normal nodes which they attributed to the presence of a well-developed Golgi apparatus. Mikata *et al.* (1968) observed acid phosphatase activity in HEV of regional nodes stimulated by typhoid vaccine and suggested that this was related to the appearance of lysosomes in the endothelium. The present study demonstrated variable cytoplasmic staining for acid phosphatase and β-glucuronidase activity in high endothelial cells of normal rat lymph nodes. Cytochemical techniques localized acid phosphatase activity within Golgi saccules and no reaction product was seen within residual lysosomes. These results did not preclude the possibility that high endothelial cells might produce lysosomal acid hydrolases following antigenic stimulation (Mikata *et al.*, 1968; Anderson *et al.*, 1975) or regional perfusion with foreign materials (Anderson, Anderson and Wyllie, 1974a). However, such changes may not be indicative of specialized HEV functions, since acid phosphatase granules have been identified in the endothelium of other blood vessels subjected to injury (Marchesi, 1964) and experimental manipulation (Hess and Staübli, 1963).

Sordat *et al.* (1971) reported that the luminal and lateral borders of high endothelial cells in human tonsils stained intensely for IgG using immunofluorescence techniques. They concluded that the accumulation of small lymphocytes within HEV walls correlated with the presence of surface immunoglobulin, and suggested that this might contribute to selective emigration of lymphocytes at this site. Use of similar unwashed, fixed tissue sections in the present study resulted in staining of high endothelial cells and plasma precipitates within lumens of HEV, arterioles and venules. However, specific staining of the lumens and endothelial surfaces of HEV was abolished by brief washing prior to fixation or use of washed, unfixed sections. Only small venules which linked capillary beds to HEV retained specific fluorescence in such preparations and no lymphocytes were seen migrating across their walls. These findings argue against specific binding of IgG on high endothelial cells and suggest that the observations by Sordat *et al.* (1971) reflect artifacts introduced by fixation.

There is circumstantial evidence indicating that the characteristic morphology and metabolic activities of HEV are related to lymphocyte traffic. HEV have been described in lymphatic tissues of all mammalian species (Miller, 1969) and at extranodal sites of chronic inflammation (Smith, McIntosh and Morris, 1970; Graham and Shannon, 1972) where intensive lymphocyte emigration occurred. The relationships between high endothelial cells and migrating lymphocytes has been debated repeatedly. Ultrastructural studies by Marchesi and Gowans (1964) suggested that lymphocytes passed directly through the cytoplasm of high endothelial cells. From this premise, other investigators (Goldschneider and McGregor, 1967; Vincent and Gunz, 1972) postulated that the unique characteristics of this endothelium reflected special transport mechanisms and membrane synthesis required for intracellular migration. While this intracellular transport hypothesis has been supported by one recent study (Farr and De Bruyn, 1975), most investigators (Schoefl, 1972; Wenk *et al.*, 1974; Anderson, Anderson and Wyllie, 1974b) have concluded that lymphocytes migrate intercellularly as they cross this endothelium. If we accept this evidence, it is possible that the specialized metabolic activities of high endothelial cells could be related to: production of chemotactic agents, synthesis of basement membrane materials to restore the basal lamina, or secretion of hydrolytic enzymes for cleansing adsorbed materials from the surfaces of migrating lymphocytes. While none of these possibilities were excluded by the present study, there was no histochemical or cytochemical evidence that acid hydrolases were emptied into extracellular spaces about migrating lymphocytes. Goldschneider and McGregor (1967) found that lymphocyte depletion produced by neonatal thymectomy or thoracic duct drainage in adult rats caused marked decreases in the volume and basophilia of high endothelial cytoplasm

which was completely reversed within 24 h by infusion with syngeneic thoracic duct lymphocytes. We could find no evidence for comparable changes in HEV in the present study where thoracic duct drainage was maintained for 8–12 days. Lymph nodes from these rats showed striking cellular depletion with markedly decreased numbers of luminal and infiltrating lymphocytes within HEV. Despite these changes, tortuous but otherwise normal HEV were seen in cleared slices of these nodes, and the high endothelial cells retained their characteristic metabolic and structural features when studied by histochemistry, light and electron microscopy. In view of these findings, it seems unlikely that reported variations in HEV during development (Söderström, 1967; Van Deurs and Röpke, 1975) and different experimental situations (Parrot, De Sousa and East, 1966; Burwell, 1962; Anderson *et al.*, 1975) can be attributed solely to changes induced by altered lymphocyte traffic. Further studies are clearly needed to document the presence and significance of specialized functions in this endothelium.

The description of HEV presented in this report may not be applicable to all mammals, since species differences have been noted in these venules (Miller, 1969). The reticular sheaths have been reported to be quite prominent in mice and rats, and barely discernible in guinea-pigs (Claësson *et al.*, 1971). In addition, the present study demonstrated that HEV structure varies in different lymphatic tissues. Within Peyer's patches, HEV formed two anastomosing venous plexuses in the interfollicular zones; no venous sphincters were seen in these vessels. HEV were lined by cuboidal endothelium which lacked apical junctional complexes and were surrounded by broad perivascular sheaths containing collagen bundles, elastic fibres and three to five layers of overlapping reticular cell plates. These features suggested that HEV in gut lymphatic tissues might be more permeable to fluids and cells. Branches of these venules frequently extended beyond the confines of the Peyer's patch to join with small blood vessels near the base of intestinal crypts. The walls and sheaths of these extralymphatic HEV were heavily infiltrated with migrating lymphocytes suggesting that they might contribute to lymphocyte traffic into the adjacent intestinal mucosa (Waksman, 1973).

ACKNOWLEDGMENTS

The authors are grateful to Miss Barbara Gould for the medical illustrations, Philip Rutledge and Raymond Lund for photographic assistance, and Phebe W. Summers for editorial assistance. We also wish to thank Dr John H. Humphrey (NIMR, Mill Hill, London) for helpful advice during the preparation of this manuscript. This study was supported in part by National Institutes of Health grants numbers HL-17596 and GM-00415 and DAMD contract number 17-74-C-4095.

REFERENCES

ANDERSON A.O. & ANDERSON N.D. (1975) Studies on the structure and permeability of the microvasculature in normal rat lymph nodes. *Amer. J. Path.* **80,** 387.

ANDERSON A.O., ANDERSON N.D. & WYLLIE R.G. (1974a) Morphologic studies on lymph node vasculature. *Amer. J. Path.* **74,** 54a.

ANDERSON A.O., ANDERSON N.D. & WYLLIE R.G. (1974b) Lymphocyte migration from high endothelial venules (HEV). *Fed. Proc.* **33,** 628.

ANDERSON N.D., ANDERSON A.O. & WYLLIE R.G. (1975) Microvascular changes in lymph nodes draining skin allografts. *Amer. J. Path.* **81,** 131.

ANTON E., BRANDES D. & BARNARD S. (1969) 'Lysosomes in uterine involution: distribution of acid hydrolyses in luminal epithelium.' *Anat. Rec.* **164,** 231.

BARKA T. (1960) A simple azo-dye method for histochemical demonstration of acid phosphatase. *Nature (Lond.),* **187,** 248.

BARKA T. & ANDERSON P.J. (1963) *Histochemistry,* p. 314. Harper & Row, New York.

BECKER C.G. & NACHMAN R.L. (1973) Contractile proteins of endothelial cells, platelets and smooth muscle. *Amer. J. Path.* **71,** 1.

BURWELL R.G. (1962) Studies of the primary and secondary immune responses of lymph nodes draining homografts of fresh cancellous bone (with particular reference to mechanisms of lymph node reactivity). *Ann. N.Y. Acad. Sci.* **99,** 821.

CLAËSSON M.H., JORGENSEN O. & RÖPKE C. (1971) Light and electron microscopic studies of the paracorticol postcapillary high-endothelial venules. *Z. Zellforsch. mikrosk. Anat.* **119,** 195.

CLARK S.L., JR (1962) The reticulum of lymph nodes in mice studied with the electron microscope. *Amer. J. Anat.* **110,** 217.

DABELOW A. (1939) Die Blutgefassversorgung der lymphatischen Organe. *Verh. Anat. Ges.* **46,** 179.

DAVIS B.J. & ORNSTEIN L. (1959) High resclution enzyme localization with a new diazo reagent, 'hexazonium pararosanaline.' *J. Histochem. Cytochem.* **7,** 297.

FARR A.G. & DE BRUYN P.P.H. (1975) The mode of lymphocyte migration through postcapillary venule endothelium in lymph nodes. *Amer. J. Anat.* **143,** 59.

FUKUDA J. (1968) Studies on the vascular architecture and the fluid exchange in the rabbit popliteal lymph node. *Keio J. Med.* **17,** 53.

GOLDSCHNEIDER I. & MCGREGOR D.D. (1967) Migration of lymphocytes and thymocytes in the rat. I. The route of migration from blood to spleen and lymph nodes. *J. exp. Med.* **127,** 155.

GOMORI G. (1939) Microtechnical demonstration of phosphatase in tissue sections. *Proc. Soc. exp. Biol. (N.Y.),* **42,** 23.

GOMORI G. (1950) Aldehyde fuchsin: a new stain for elastic tissue. *Amer. J. clin. Path.* **20,** 665.

GOWANS J.L. (1959) The recirculation of lymphocytes from blood to lymph in the rat. *J. Physiol.* **146,** 54.

GOWANS J.L. & KNIGHT E.J. (1964) The route of re-circulation of lymphocytes in the rat. *Proc. roy. Soc.* B, **159,** 257.

GRAHAM R.C., JR & SHANNON S.L. (1972) Peroxidase arthritis. II. Lymphoid cell-endothelial interactions during a developing immunologic inflammatory response. *Amer. J. Path.* **69,** 7.

HAYASHI M., NAKAJIMA Y. & FISHMAN W.N. (1964) The cytological demonstration of β-glucuronidase employing naphthol AS-BI glucuronide and hexazonium pararosaniline. *J. Histochem. Cytochem.* **12,** 293.

HESS R. & STAÜBLI W. (1963) The development of aortic lipidosis in the rat. A correlative histochemical and electron microscopic study. *Amer. J. Path.* **43,** 301.

HUMMEL K.P. (1935) The structure and development of the lymphatic tissue in the intestine of the albino rat. *Amer. J. Anat.* **57,** 351.

JORGENSEN O. & CLAËSSON M.H. (1972) Studies on the post-capillary high endothelial venules of neonatally thymectomized mice. *Z. Zellforsch. mikrosk. Anat.* **132,** 347.

LEAK L.V. & BURKE J.F. (1968) Ultrastructural studies on the lymphatic anchoring filaments. *J. Cell Biol.* **36,** 129.

MARCHESI V.T. (1964) Some electron microscopic observations on interactions between leukocytes, platelets, and endothelial cells in acute inflammation. *Ann. N.Y. Acad. Sci.* **116,** 774.

MARCHESI V.T. & GOWANS J.L. (1964) The migration of lymphocytes through the endothelium of venules in lymph nodes: an electron microscope study. *Proc. roy. Soc.* B, **159,** 283.

MIKATA A., NIKI R. & WATANABE S. (1968) Reticuloendothelial system of the lymph node parenchyma, with special reference to post-capillary venules and granuloma formation. *Rec. Advanc. R.E.S. Res.* **8,** 143.

MILLER J.J., III (1969) Studies of the phylogeny and ontogeny of the specialized lymphatic tissue venules. *Lab. Invest.* **21,** 484.

NOVIKOFF A.B., ESSNER E., GOLDFISCHER S. & HEUS M. (1962) Nucleoside phosphatase activity of cytomembranes *Symp. internat Soc. cell. Biol.* **1,** 149.

PARROT D.M.V., DE SOUSA M.A.B. & EAST J. (1966) Thymus-dependent areas in the lymphoid organs or neonatally thymectomized mice. *J. exp. Med.* **123,** 191.

PRESSMAN J.J., SIMON M.B., HAND K. & MILLER J. (1962) Passage of fluids, cells and bacteria via direct communications between lymph nodes and veins. *Surg. Gynec. Obstet.* **114,** 207.

ROMANUL F.C.A. & BANNISTER R.G. (1962) Localized areas of high alkaline phosphatase activity in the terminal arterial tree. *J. Cell Biol.* **15,** 78.

RÖPKE C., JORGENSEN O. & CLAËSSON M.H. (1972) Histochemical studies of high-endothelial venules of lymph nodes and Peyer's patches in the mouse. *Z. Zellforsch. mikrosk. Anat.* **131,** 287.

SCHOEFL G.I. (1972) The migration of lymphocytes across the vascular endothelium in lymphoid tissue. *J. exp. Med.* **136,** 568.

SCHULZE W. (1925) Untersuchungen über die Vapillären and postcapillären Venen lymphatischer Organe. *Z. Anat. Entwicklungsgesch.* **76,** 421.

SCHUMACHER S.V. (1899) Ueber Phagocytose und die Abfuhrwege der Leucocyten in den Lymphdrüsen. *Arch. mikrosk. Anat.* **54,** 311.

SMITH C. & HENON B.K. (1959) Histological and histochemical study of high endothelium of post-capillary veins of the lymph node. *Anat. Rec.* **135,** 207.

SMITH J.B., MCINTOSH G.H. & MORRIS B. (1970) The migration of cells through chronically inflamed tissues. *J. Path.* **100,** 21.

SÖDERSTRÖM N. (1967) Post-capillary venules as basic structural units in the development of lymphoglandular tissue. *Scand. J. Haemat.* **4,** 411.

SORDAT B., HESS M.W. & COTTIER H. (1971) IgG immunoglobulin in the wall of post-capillary venules: possible relationship to lymphocyte recirculation. *Immunology,* **20,** 115.

SUGIMURA M. (1964) Fine structure of post-capillary venules in mouse lymph nodes. *Jap. J. vet. Res.* **12,** 83.

TAKAMATSU H. (1939) Histologische und biochemische Studien über die Phosphatase. I. Histochemische Untersuchungsmethodik Phosphatase und deren Verteilung in verschiedenen Organen und Geweben. *Trans. Soc. Path. Jap.* **29,** 492.

THOMÉ R. (1898) Endothelien als Phagocyten (aus den Lymphdrüsen von Macacus cynomolgus). *Arch. mikrosk. Anat.* **52,** 820.

VAN DEURS B. & RÖPKE C. (1975) The postnatal development of high-endothelial venules in lymph nodes of mice. *Anat. Rec.* **181,** 659.

VINCENT P.C. & GUNZ F.W. (1970) Control of lymphocyte level in the blood. *Lancet,* **ii,** 342.

WACHSTEIN M. & MEISEL E. (1957) Histochemistry of hepatic phosphatases at a physiologic pH. *Amer. J. clin. Path.* **27,** 13.

WAKSMAN B.H. (1973) The homing pattern of thymus-derived lymphocytes in calf and neonatal mouse Peyer's patches. *J. Immunol.* **111,** 878.

WENK E.J., ORLIC D., REITH E.J. & RHODIN J.A.G. (1974) The ultrastructure of mouse lymph node venules and the passage of lymphocytes across their walls. *J. Ultrastruct. Res.* **47,** 214.